Bacterial interspecies interactions modulate pH-mediated antibiotic tolerance in a model gut microbiota

Andrés Aranda-Díaz[1], Benjamin Obadia[2], Tani Thomsen[1], Zachary F. Hallberg[3], Zehra Tüzün Güvener[2], Kerwyn Casey Huang[1,4,5,*], William B. Ludington[2,6,*]

[1]Department of Bioengineering, Stanford University, Stanford, CA 94305, USA

[2]Department of Molecular and Cell Biology, University of California, Berkeley, Berkeley, CA 94720, USA

[3]Department of Plant and Microbial Biology, University of California, Berkeley, Berkeley, CA 94720, USA

[4]Department of Microbiology and Immunology, Stanford University School of Medicine, Stanford, CA 94305, USA

[5]Chan Zuckerberg Biohub, San Francisco, CA 94158

[6]Department of Embryology, Carnegie Institution of Washington, Baltimore, MD 21218

[*]To whom correspondence should be addressed: kchuang@stanford.edu, ludington@carnegiescience.edu

Abstract

Despite decades of investigation into how antibiotics affect isolated bacteria, it remains highly challenging to predict consequences for communities in complex environments such as the human intestine. Interspecies interactions can impact antibiotic activity through alterations to the extracellular environment that change bacterial physiology. By measuring key metabolites and environmental pH, we determined that metabolic cross-feeding among members of the fruit fly gut microbiota drives changes in antibiotic sensitivity *in vitro*. Co-culturing of *Lactobacillus plantarum* with *Acetobacter* species induced tolerance to rifampin. Mechanistically, we found that acetobacters counter the acidification driven by *L. plantarum* production of lactate, and that pH shifts during stationary phase were sufficient to drive rifampin tolerance in *L. plantarum* monocultures. The key *Lactobacillus* physiological parameter related to tolerance was a reduction in lag time exiting stationary phase, opposite to a previously identified mode of tolerance to ampicillin in *E. coli*. *Lactobacillus* tolerance to erythromycin also depended on growth status and pH, suggesting that our findings generalize to other antibiotics. Finally, tolerance of *L. plantarum* to rifampin varied spatially across the fruit fly gut. This mechanistic understanding of the coupling among interspecies interactions, environmental pH, and antibiotic tolerance enables

39 future predictions of growth and the effects of antibiotics in more complex

40 communities and within hosts.

Introduction

Decades of investigations have described detailed and precise molecular mechanisms of antibiotic action in model organisms. Yet, our current understanding is biased by a narrow set of standardized laboratory conditions; a recent study reported that resistance of *Escherichia coli* to the beta-lactam mecillinam is rarer in clinical isolates than in the laboratory and involves distinct genetic loci[1]. Unlike in laboratory monocultures, the vast majority of bacteria live in diverse communities such as the human gut microbiota. Antibiotics impact gut communities in many ways, ranging from the loss of diversity[2,3] to the evolution of multidrug-resistant gut pathogens[4]. Hence, there is a pressing need for new frameworks that predict how antibiotics affect bacterial communities.

Bacteria can survive antibiotics through (i) resistance mutations, which counteract the antibiotic mechanism; (ii) persistence, whereby a subset of the bacterial population survives the antibiotic by becoming metabolically dormant; or (iii) tolerance, whereby the entire population enters an altered physiological state that is not susceptible to the antibiotic[5]. Members of multispecies communities, such as biofilms and models of urinary tract infections, can display altered sensitivity to antibiotics[6-9]. A few studies have delved into the molecular mechanisms behind cross-species antibiotic protection and sensitization. For

example, the exoproducts of *Pseudomonas aeruginosa* affect the survival of *Staphylococcus aureus* through changes in antibiotic uptake, cell-wall integrity, and intracellular ATP pools[10]. In synthetic communities, intracellular antibiotic degradation affords cross-species protection against chloramphenicol[11]. Additionally, metabolic dependencies within synthetic communities can lower the viability of bacteria when antibiotics eliminate providers of essential metabolites, leading to an apparent change in the minimum inhibitory concentration (MIC) of the dependent species[9]. However, we still lack understanding of how contextual metabolic interactions between bacteria affect the physiological processes targeted by antibiotics and the resulting balance between growth inhibition (bacteriostatic activity) and death (bactericidal activity).

Characterizing the impact of metabolic interactions on antibiotic susceptibility requires functional understanding of how bacterial species interact during normal growth. Interspecies interactions can occur through specific mechanisms within members of a community (e.g. cross-feeding or competition for specific resources), or through global environmental variables modified by bacterial activity. An example of the latter is pH, which has recently been shown to drive

80 community dynamics in a highly defined laboratory system of decomposition
81 bacteria[12].
82
83 While synthetic communities afford the opportunity to design and to tune
84 bacterial interactions, it is unclear whether findings are relevant to natural
85 communities. The stably associated gut microbiota of *Drosophila melanogaster* fruit
86 flies constitutes a naturally simple model community for determining how
87 metabolic interactions between species affect growth, physiology, and the action
88 of antibiotics[13]. This community consists of ~5 species predominantly from the
89 *Lactobacillus* and *Acetobacter* genera[14] (Fig. 1a). Lactobacilli produce lactic acid[15],
90 while acetobacters are acetic acid bacteria that are distinguished by their ability
91 to oxidize lactate to carbon dioxide and water[16]. Short chain fatty acids, such as
92 lactate, decrease the pH of natural fermentations and may constitute a
93 mechanism through which pH plays a prominent role in community dynamics.
94 The naturally low number of species in *Drosophila* gut microbiota and its
95 compositional modularity (lactobacilli versus acetobacters) enable systematic
96 dissection of microbial interactions.
97
98 In the current study, we interrogated how interspecies interactions affect growth
99 and antibiotic susceptibilities. We used high-throughput assays to measure these

parameters in monocultures versus co-cultures and inside fly guts. *Lactobacillus plantarum* (*Lp*) exhibited antibiotic tolerance (delay in death[5] by ~12 h) in the presence of acetobacters. Lactate accumulation by *Lp* in monocultures acidified the media, inhibiting growth during stationary phase. *Acetobacter*-mediated lactate consumption released this inhibition by increasing pH, leading to a shorter *Lp* lag while exiting stationary phase. This reduced lag exiting stationary phase corresponded with the antibiotic tolerance of *Lp* that we observed. We determined that changes in pH elicited by *Acetobacter* activity are sufficient to modulate tolerance of *Lp* to both rifampin and erythromycin. Finally, *ex vivo* experiments revealed that antibiotic tolerance differs in distinct compartments of the host gastrointestinal tract. Taken together, our findings indicate that simple changes to the environment can drive complex behaviors within bacterial communities.

Results

Interspecies interactions induce tolerance to rifampin

To determine the composition of the gut microbiota in our laboratory fruit flies, we performed deep sequencing of 16S rRNA V4 amplicons from 18 individual dissected guts (Methods). We identified five species belonging to seven unique operational taxonomic units (OTUs) by clustering the sequences at 99% identity: *L. plantarum* (*Lp*), *L. brevis* (*Lb*), *Acetobacter pasteurianus* (*Ap*), *A. tropicalis* (*At*), and *A. aceti* (*Aa*) (Fig. 1a). We then isolated the species in culture and determined the antibiotic sensitivities of the four major fly gut inhabitants (*Lp*, *Lb*, *Ap* and *At*; Fig. 1a) *in vitro* using isolates of these species (Table S1) grown in Man, Rogosa, and Sharpe (MRS) medium. We tested 10 antibiotics representing a wide variety of classes using plate-based growth assays (Methods). For many drugs, some of the fly gut species were resistant (detectable growth) at least up to the highest concentrations tested. Rifampin was the only drug for which all four species exhibited sensitivity (Table S2) and it is bactericidal[17], hence there is the opportunity to study survival as well as sensitivity.

We noted from growth curves in the absence of drug that *Lb* grew significantly more slowly than *Lp* (0.60 ± 0.054 h^{-1} vs. 0.64 ± 0.001 h^{-1} for *Lp*, $P = 5.5\times10^{-3}$, $n = 16$,

Fig. S1) and had a much longer lag phase than *Lp* (6.55 ± 0.16 h vs. 1.92 ± 0.08 h for *Lp*, $P = 1.8\times10^{-39}$, $n = 16$, Fig. S1). Thus, we focused on *Lp* and its interactions with the *Acetobacter* species, particularly *Ap*, which is more abundant in the fly gut than the other acetobacters (Fig. 1a).

We grew *Lp* and *Ap* separately for 48 h in test tubes, combined them in test tubes at an optical density at 600 nm (henceforth OD) of 0.02 each, and co-cultured them in MRS for 48 h. We then diluted this co-culture and 48-h monocultures of *Lp* and *Ap* into fresh MRS at ~5×10^5 colony-forming units/mL (CFU/mL) in 96-well plates with various concentrations of rifampin and measured growth over 48 h. The MIC of the co-culture was similar to that of *Lp* alone (2.5 μg/mL, Fig. S2a). To determine whether the co-culture still contained both species, we measured the percentage of survival and the fraction of each species at various rifampin concentrations by taking advantage of the fact that *Lp* and the acetobacters have distinct colony morphologies and colors on MRS and MYPL plates (Table S1). We measured *Lp* CFUs on MRS and *Ap* CFUs on MYPL because *Lp* and *Ap* grow more quickly on MRS and MYPL, respectively. In the co-culture, *Ap* died off at a similar concentration of rifampin as during growth in a monoculture (1.25 μg/mL, Fig. S2b). For *Lp*, the MIC was the same in co-culture as in monoculture (1.25 μg/mL, Fig. 1b), but at concentrations above the MIC,

154 significantly more *Lp* cells survived in co-culture than in monoculture (Fig. 1b).
155 This effect could not be explained by small differences in the initial inoculum, as
156 increasing cell densities up to 100-fold did not change the MIC or survival of *Lp*
157 in monoculture (Fig. S2c,d). Because of the change in *Lp* survival, we focused
158 herein on this phenotype.
159
160 To determine whether *Lp*'s increased survival was specific to co-culturing with
161 *Ap*, we co-cultured *Lp* with each of the acetobacters, including a wild fly isolate
162 of *A. indonesiensis* (*Ai*), and lab fly isolates of *A. orientalis* (*Ao*) and *Aa*, the fifth
163 major component of the microbiota of our flies (Fig. 1a). We then diluted each co-
164 culture to an initial *Lp* cell density of ~5×10^5 CFU/mL into fresh MRS with 20
165 μg/mL rifampin (16X MIC) and let the cells grow for 24 h. Co-culturing with any
166 of the acetobacters increased survival by approximately one order of magnitude
167 (Fig. 1c). To determine whether this increased survival requires co-culturing
168 prior to rifampin treatment (rather than the presence of the acetobacters being
169 sufficient), we grew *Lp* and *Ap* separately for 48 h and mixed and diluted them at
170 the time of addition of 20 μg/mL rifampin. After 24 h of growth, the number of
171 CFU/mL was significantly lower in mixed culture than in co-culture (Fig. 1d),
172 indicating a history dependence to increased survival.
173

174 To determine whether co-culturing slows killing by the drug, we examined the
175 survival of *Lp* over time at a high drug concentration (50 μg/mL, 40X MIC).
176 Similar to the experiments above, we compared *Lp* CFU/mL in a monoculture
177 with that in a co-culture with *Ap*. In monoculture, *Lp* rapidly died, with CFU/mL
178 becoming undetectable within 18 h; in contrast, *Lp* survived >30 h after co-
179 culturing (Fig. 1e). This increased time to death of *Lp* as a bulk population, and
180 unchanged MIC, together indicate that co-culturing *Lp* with *Ap* induces tolerance
181 of *Lp* to rifampin[5].
182
183 *Co-culturing leads to growth of* Lp *in stationary phase*
184 Our finding that co-culturing *Lp* with acetobacters affects antibiotic tolerance
185 (Fig. 1c,e) prompted us to investigate the environmental factors that cause this
186 phenotype. We first inquired whether the total amount of growth of the co-
187 culture was larger or smaller than expected from the yield of the monocultures.
188 We grew *Lp* and each of the acetobacters separately for 48 h, diluted the
189 monocultures to OD = 0.04, combined the *Lp* monoculture 1:1 with each
190 *Acetobacter* monoculture, and grew the co-cultures for 48 h in test tubes. In bulk
191 measurements, the *Lp-Ap* co-culture showed a significant synergistic effect
192 (Supplementary Text, Fig. S3a). We then determined the total carrying capacity
193 of each of the species in the co-cultures grown in test tubes by counting CFUs.

We determined that the *Lp* CFU/mL values for 48-h co-cultures with *Ap*, *At*, and *Ai* were higher than the *Lp* CFU/mL values in monoculture (Fig. 2a). Co-cultures with *Ap* showed the strongest effect; *Aa* and *Ao* did not significantly increase *Lp* CFU/mL (Fig. 2a). All acetobacters except for *Ap* reached lower CFU/mL in co-cultures with *Lp* than in monocultures (Fig. S3b). Thus, *Lp* has a strong positive interaction with *Ap*, and negative or neutral interactions with the rest of the acetobacters (Supplementary Text, Fig. S3c).

To determine when the additional growth took place, we monitored CFU/mL values for *Lp* and *Ap* in co-culture throughout a 48-h time course starting from an initial combined cell density of ~5×10^5 CFU/mL. Initially, *Lp* accounted for the bulk of the growth in the co-culture (Fig. 2b). Interestingly, *Ap* in liquid monoculture showed little to no growth in most replicates after 40 h (Fig. 2b); by contrast, in liquid co-culture *Ap* started to grow after ~20 h and reached saturation by ~40 h (Fig. 2b), indicating that *Ap* also benefited from growth as a co-culture. This benefit likely stemmed from a reduction in *Ap* cell death during lag phase (Supplementary Text, Fig. S4). Thus, a mutualism exists between *Lp* and *Ap* driven by growth during and exiting from stationary phase.

Lactate metabolism leads to changes in pH in stationary phase co-cultures

214 Interestingly, after 30 h, *Lp* displayed a significant (~2X) increase in CFU/mL in
215 the co-culture that did not occur in the monoculture (Fig. 2b), indicating that the
216 increase in final yield occurs late in stationary phase. We therefore hypothesized
217 that *Lp* has a common metabolic interaction with each of the acetobacters. An
218 obvious candidate is cross-feeding, since *Lp* produces lactate and the acetobacters
219 consume it. We measured lactate levels in the supernatants of *Lp* monocultures
220 and co-cultures of *Lp* with each of the acetobacters individually, after 48 h of
221 growth. As expected, the Lp monoculture accumulated L- and D-lactate to high
222 levels (>100 mM; Fig. 2c). All co-cultures had significantly lower concentrations
223 of both isomers than the monoculture (<2 mM, Fig. 2c). The *Lp-Ao* co-culture
224 harbored higher levels of L-lactate than any other co-culture and *Lp-Aa* had
225 higher concentration of L-lactate than the rest of the co-cultures (Fig. 2c). *Lp-Ap*,
226 *Lp-Ao*, and *Lp-Aa* co-cultures all accumulated lactate (>10 mM) at 20 h (Fig. S5a).
227 Taken together, these data suggest that *Lp* metabolism leads to an initial
228 accumulation of lactate and that the acetobacters consume it, although *Aa* and *Ao*
229 are less efficient at consuming L-lactate than the other species.
230
231 Since lactate is a short-chain fatty acid with a pK_a of 3.86, we suspected that
232 lactate production would affect the pH of the culture. We first monitored the pH
233 dynamics of monocultures of *Lp* and of each *Acetobacter* using the pH-sensitive

fluorophore 2',7-bis-(2-carboxyethyl)-5-(and-6)-carboxyfluorescein (BCECF)[18]. In the *Lp* monoculture, pH decreased from pH=6.75 to below 4 during growth (Fig. 2d); more precisely, we measured a final supernatant pH=3.77 using a pH meter (Fig. S5a). We measured pH over time in *Acetobacter* monocultures using BCECF. For all acetobacters except *Ap*, the medium first acidified down to pH~5, and then increased back to pH=6-7 (Fig. 2d).

To test whether acetobacters reverse the pH decrease due to the accumulation of lactate produced by *Lp*, we measured the pH of co-cultures over time using BCECF. Co-cultures with *Ap*, *At*, and *Ai* followed similar trajectories in which the pH followed that of the *Lp* monoculture for the first 20 h, after which the pH increased up to a final value of ~7 (Fig. 2f). The *Lp-Aa* co-culture experienced a ~10-h delay in the pH increase, while the co-culture with *Ao* showed only a slight pH increase by 48 h (Fig. 2f). The slight pH increase in *Ao* co-culture is consistent with lower L-lactate consumption by this species (Fig. 2c). Using a pH meter for validation, we measured final pH values of 5.9, 5.8, 4.6, 5.4, and 4.8 in co-cultures with *Ap*, *At*, *Ao*, *Ai*, and *Aa*, respectively (Fig. S5b). Thus, lactate metabolism dictates dramatic shifts in environmental pH that are related to physiological changes in antibiotic tolerance (Fig. 1c).

Given the strong acidification of the medium in *Lp* monoculture but not in co-culture (Fig. 2d), we hypothesized that intracellular pH decreases in monoculture and increases in co-culture. To measure intracellular pH, we transformed our *Lp* strain with a plasmid expressing pHluorin (a GFP variant that acts as a ratiometric pH sensor[19]) under the control of a strong constitutive promoter[20]. The two absorbance peaks, which we measured at 405 and 475 nm, are sensitive to pH and the ratio of the emission (at 509 nm) at these two excitation wavelengths can be used to estimate intracellular pH. We grew this strain in monoculture and in co-culture with *Ap* and measured fluorescence over time in a plate reader. Because of the high autofluorescence of the medium at 405 nm (data not shown), we could only track changes in fluorescence at an excitation wavelength of 475 nm. We observed an initial increase in signal as the *Lp* cells started to proliferate (Fig. S6a). After the cultures saturated (t~20 h), we detected a decrease in the signal down to the levels of medium autofluorescence in the monoculture (Fig. S6a). In the co-culture, where the extracellular pH is raised by the metabolic activity of *Ap*, fluorescence did not decrease over time (Fig. S6a), suggesting that intracellular pH decreases in a time-dependent manner in monoculture but not in co-culture.

To verify that the decrease in fluorescence in monoculture was due to a drop in intracellular pH, as opposed to a decrease in protein synthesis, we sampled cells after 48 h of growth, centrifuged them, resuspended them in PBS in order to measure pHluorin signal at both its excitation wavelengths, and measured fluorescence within 1 minute of resuspension. The ratio of the signal from pHluorin at its two excitation wavelengths was significantly higher in co-culture (Fig. S6b). Taken together, these data indicate that the intracellular pH of *Lp* cells is significantly lower in monoculture than in co-culture with acetobacters.

Low pH inhibits the growth of Lp *and extends lag phase*

Since *Ap* growth causes a large increase in the extracellular pH of an *Lp-Ap* co-culture, we sought to determine the dependence of *Lp* growth on pH. We diluted a 48-h culture of *Lp* cells grown in MRS at starting pH=6.75, to a starting OD=0.02 in MRS adjusted to starting pH ranging from 3 to 8 (Methods). We then measured growth and BCECF fluorescence in a plate reader (Fig. S7a,b). For lower starting pH values, the carrying capacity was lower (Fig. 3a) and varied over a large OD range from <0.02 to >2. For all starting pH values, *Lp* cells reduced the pH to a common final value of ~3.7 (Fig. 3a). The bulk growth rate approached zero (Fig. 3b) as the pH approached its final value, explaining the

differences in yield. Interestingly, the maximum growth rate was also pH-dependent (Fig. 3c), with the highest growth rate at starting pH=7.

Given these findings, we hypothesized that the inhibition of growth in stationary phase of an *Lp* monoculture is due to the decreased intracellular and extracellular pH, and that *Ap* releases *Lp*'s growth inhibition by raising intracellular and extracellular pH. To test this hypothesis, we inoculated a 48-h culture of *Lp* to an initial OD=0.02 into the supernatant of a 48-h *Lp* culture at pH=3.77 or set to pH=7. We observed substantially more growth (~20-fold increase) of the bulk culture in supernatant raised to pH=7, while no growth took place starting from pH=3.77 (Fig. 3d). As expected, the maximal growth rate was lower than in fresh MRS due to the partial depletion of nutrients (Fig. 3d); addition of glucose to the conditioned medium supported faster growth, but only starting from neutral pH (Fig. S7c). We also hypothesized that the accumulation of lactate by *Lp* would allow growth of *Ap* in *Lp*-conditioned medium even at low starting pH. When we diluted a saturated *Ap* culture into *Lp*-conditioned medium generated as above, *Ap* grew to similar levels as in fresh MRS (Fig. S7d).

These findings suggested that the effects of *Ap* in co-culture on *Lp* growth might be due primarily to the pH changes that *Ap* initiates because of the ability of

312 acetobacters to grow at low pH and to consume lactate. Thus, we first increased
313 the pH of an *Lp* monoculture to 7 after 30 h, when the pH increased most rapidly
314 in the *Lp-Ap* co-culture (Fig. 3e), and incubated cells for an additional 18 h. We
315 did not observe a significant increase in CFU/mL from this pH-adjusted culture
316 versus controls that simply grew for 48 h or were subjected to all washes
317 required for pH adjustment and then returned to the same supernatant (Fig. S7e).
318 We then assessed if increasing the pH at 30 h resulted in a decrease in the
319 duration of lag phase by diluting the monoculture to OD=0.0375 into fresh MRS
320 after an additional 18 h of growth. The lag phase was shorter in the pH-adjusted
321 culture than control bulk cultures (Fig. 3e). Thus, pH is a driver of the growth
322 advantages of *Lp* in lag phase.
323
324 *Co-culturing* Lp *with acetobacters reduces lag time*
325 Canonical antibiotic tolerance in *E. coli* results from a decrease in growth rate or
326 an increase in lag phase that protects cells through metabolic inactivity[5]. To
327 measure growth rate and lag phase, we co-cultured *Lp* with each of the
328 acetobacters individually for 48 h, diluted the culture to a common OD of 0.0375,
329 and monitored growth in a plate reader. The maximum growth rate was the
330 same for the *Lp* monoculture and co-cultures with *Ap*, *At*, and *Ai*, and slightly
331 higher for co-cultures with *Ao* and *Aa* (Fig. S8). We previously observed for *Lp*

monocultures when shifting the pH that the stimulation of growth in stationary phase was connected with tolerance (Fig. 3e), opposite to that of *E. coli* tolerance to ampicillin[5]. In agreement with these data, there was a significant decrease in bulk lag time for all of the *Acetobacter* co-cultures (Fig. 4a,b). *Ap*, *At*, and *Ai* co-cultures had the largest lag decreases. The *Aa* and *Ao* co-cultures had a smaller, although still significant, decrease (Fig. 4a,b); interestingly, *Aa* and *Ao* were also less efficient at consuming lactate than the other *Acetobacter* species (Fig. 2c). These data indicate that interspecies interactions can change the physiology of the community, and that differences across the acetobacters constitute an opportunity to probe the underlying cause of the lag phenotype.

As with *Lp* tolerance to antibiotics (Fig. 1b), the shortened lag phase of the *Lp-Ap* co-culture was history dependent. When we mixed 48-h cultures of *Lp* and *Ap* to a combined initial OD of 0.0375 in the absence of antibiotics, the resulting bulk culture had the same lag time as an *Lp* monoculture (Fig. 4c,d). To determine which of the two species was responsible for the decrease in lag, we diluted a 48-h co-culture of *Lp* and *Ap* 1:200, spotted 2 μL onto a 1% agarose + MRS pad, and performed time-lapse microscopy (Methods) to monitor the initiation of growth at the single-cell level (Fig. 4e). *Lp* and *Ap* are clearly distinguishable based on morphology (Fig. S9): *Lp* cells are longer (2.46 ± 0.78 μm vs. 1.66±0.38 μm) and

thinner (0.72 ± 0.12 μm vs. 0.90 ± 0.09 μm) than *Ap* cells. Therefore, we used the aspect ratio (length/width; 3.41 ± 0.91 for *Lp* and 1.87 ± 0.46 for *Ap*) to distinguish single cells from each species in co-culture. We validated this strategy on co-cultures of fluorescently tagged strains of the same two species and observed a 10% error rate in classification (Fig. S9d-f). In co-culture, most *Lp* cells were observed to have grown by 1 h after spotting, but in *Lp* monoculture, few cells were growing even after 2 h (Fig. 4e,f). *Ap* cells did not grow during the time of imaging (Fig. 4f), indicating that the reduced lag time was due to *Lp*'s growth, in agreement with CFU/mL measurements (Fig. 2b).

Growth status and pH are drivers of antibiotic tolerance

Since pH changes shortened lag phase (Fig. 3e), and since changes in lag time were related to antibiotic tolerance (Fig. 1,4), we tested whether shortening lag phase was sufficient to induce tolerance. Lag phase can be manipulated by increasing time in starvation[21]. To determine the relationship between time spent in stationary phase and lag time in *Lp*, we diluted a 48-h monoculture to a starting OD=0.02 in fresh medium and grew it for varying amounts of time. We then diluted these monocultures into fresh medium at OD=0.0375 and measured bulk culture growth in a plate reader. Incubating the *Lp* monocultures for more

371 than 48 h resulted in a dramatic increase in the duration of lag phase, while
372 reducing the culturing time shortened lag phase (Fig. 5a).
373
374 Because lag phase in co-culture is slightly shorter than that of a 24-h monoculture
375 (Fig. 5a), we decided to match the lag time of a co-culture by growing a
376 monoculture for 20 h from an initial OD=0.02. We then measured *Lp* survival in
377 20 μg/mL rifampin after 24 h in cultures diluted from a 48-h-old or a 20-h-old
378 culture. Culturing for 20 h resulted in a significant increase in survival (Fig. 5b).
379 We next tested whether shortening lag phase by changing the pH in stationary
380 phase also yielded increased rifampin tolerance of *Lp* in co-culture. We increased
381 the pH of an *Lp* monoculture to 7 after 30 and 40 h, and grew cells for an
382 additional 18 h and 8 h, respectively. We then measured the change in CFU/mL
383 upon treatment with 50 μg/mL rifampin for 24 h. The upshift in pH at t = 30 h or
384 40 h resulted in increased tolerance relative to the unshifted monoculture (Fig.
385 5c). To test the extent to which changes in pH affect tolerance, we grew co-
386 cultures of *Lp* and *Ap* for a total of 48 h and decreased the pH to 3.7 at t = 30 h or
387 40 h. In both cases, the viability after 24 h of rifampin exposure was significantly
388 reduced relative to an untreated monoculture (Fig. 5d). Thus, pH can affect
389 tolerance both positively and negatively.
390

391 In co-culture with *Lp*, *Ap* raised the pH earlier than did *Aa*, while *Ao* only raised
392 the pH very slightly (Fig. 2d). We hypothesized that due to these distinct pH
393 dynamics, rifampin would also have different killing *Lp* dynamics in these co-
394 cultures. We grew co-cultures of these acetobacters with *Lp* as previously, and
395 then treated the co-cultures with 50 μg/mL rifampin. While all co-cultures had
396 extended survival relative to *Lp* monoculture, the killing dynamics of *Lp* were
397 indeed distinct, with *Aa* inducing the highest tolerance (Fig. 5e). To determine
398 the extent to which these dynamics can be explained by the time at which each
399 species raises the pH, we measured CFU/mL at various time points after
400 rifampin treatment for *Lp* monocultures grown for 48 h whose pH was raised to
401 pH 7 at t = 30 h or 40 h, mimicking the early and late increases in pH for *Ap* and
402 *Aa* co-cultures, respectively. The shift to pH 7 at 40 h induced higher rifampin
403 tolerance than the shift at 30 h (Fig. 5f), consistent with the increased tolerance of
404 the *Lp*-*Aa* co-culture (Fig. 5e). Moreover, shifting the pH to 4.5 at t = 30 h, to
405 mimic the slight increase caused by *Ao*, was also sufficient to increase tolerance
406 comparable to pH neutralization at t = 30 h (Fig. 5f), consistent with the similar
407 killing dynamics of the *Ap* and *Ao* co-cultures (Fig. 5e). All pH shifts induced
408 higher tolerance compared to control cultures that underwent the same protocol
409 but whose pH was maintained (Fig. 5f). Taken together, these experiments

410 establish that pH changes drive the tolerance of *Lp* to rifampin through changes
411 in the exit from stationary phase.
412
413 *Growth status and pH also drive tolerance to a ribosome-targeting antibiotic*
414 The robust relationships among changes in pH, lag time, and rifampin tolerance
415 prompted us to explore how changes in pH and lag time affect survival to other
416 antibiotics. We decided to use the ribosome-targeting macrolide erythromycin
417 because it is bactericidal and *Lp* is sensitive to it (Table S2). We treated *Lp*
418 monocultures grown for 20 h or 48 h with increasing concentrations of
419 erythromycin for 24 h at a starting cell density of ~5×10^5 CFU/mL. In contrast to
420 our observations with rifampin (Fig. 5b), a 48-h *Lp* monoculture displayed
421 tolerance to erythromycin, while a 20-h culture did not (Fig. 5g). While both
422 cultures had the same MIC in erythromycin (0.078 μg/mL, Fig. 5g), at
423 concentrations above the MIC, the 48-h culture showed no changes in CFU/mL
424 after 24 h of erythromycin treatment; the 20-h culture had a reduction of ~10-fold
425 in CFU/mL (Fig. 5g). This result suggests that *Lp* cells diluted from a 48-h culture
426 are tolerant to erythromycin, opposite to the effect we observed with rifampin.
427
428 To further determine whether antibiotic tolerance underlies the survival of *Lp* to
429 erythromycin as well as to rifampin, we diluted 20- and 48-h cultures to a

starting density of ~5×10^5 CFU/mL, exposed them to a high concentration of erythromycin (2 μg/mL, 25X MIC), and monitored CFU/mL over time. Cells from a 20-h culture died significantly more rapidly than cells from a 48-h-old culture (Fig. 5h), indicating that the differences in survival (Fig. 5g) are explained by erythromycin tolerance. Further, increasing the pH of an *Lp* monoculture at 30 h and then exposing it after an additional 18 h of growth to 2 μg/mL erythromycin in fresh medium had an increase in the rate of killing that was similar to that achieved with a 20-h culture (Fig. 5h). These results highlight that the effects of changing the growth status of a culture by different means are not limited to rifampin and—as in the case of erythromycin—can be opposite.

Growth state in the fruit fly gut determines antibiotic tolerance ex vivo

Our *in vitro* observations connecting changes in pH to lag time and antibiotic tolerance prompted us to examine whether these properties are also linked within the fruit fly gut. This tract consists of a ~5-mm-long tube divided into three sections: foregut, midgut, and hindgut (Fig. 5i). The foregut includes an accessory storage organ known as the crop. The contents of the crop are delivered to the midgut through the proventriculus and transit through the midgut to end in the hindgut, where they are expelled into the environment through the rectum and the anus[22]. Specialized "copper" cells in the central

450 portion of the midgut keep the pH of this section low, akin to the stomach in
451 mammals[23]. Bacteria are distributed along the *Drosophila* gastrointestinal tract; *Lp*
452 in particular can colonize all compartments with slight variations in its
453 distribution along the tract[24].
454
455 To examine whether variations along the fly gut impact *Lp* physiology, we
456 coarse-grained the digestive tract into the crop and the midgut and quantified
457 rifampin tolerance of *Lp* from these regions. We hypothesized that the different
458 functions of these regions – storage, or nutrient absorption and transit – lead to
459 differences in bacterial physiology. We colonized 5-7-day-old, female, germ-free
460 flies with *Lp* and left them for three days in sterile food to reach equilibrium
461 (Methods). We then dissected the flies and separated the crop from the midgut.
462 We pooled (i) dissected crops and (ii) dissected midguts in MRS to obtain a final
463 bacterial density of ~5×10^5 CFU/mL. Crops had overall ~10 times less *Lp* than the
464 midgut (8,700 CFU/crop vs. 86,000 CFU/midgut). After homogenization, the
465 samples were exposed to 20 μg/mL or 50 μg/mL rifampin for 24 h. The MIC of
466 rifampin for these *ex vivo* samples was approximately the same as for *in vitro*
467 cultures (1.25 μg/mL). For cultures extracted from the crop, significantly more
468 cells survived than for cultures extracted from the midgut, with values
469 comparable to those of a co-culture with *Ap* and a monoculture, respectively (Fig.

470 5j). These results indicate that spatial heterogeneity in the host can lead to

471 differences in the duration of lag phase and antibiotic tolerance *ex vivo*.

Discussion

Our measurements of the growth behavior of the fly gut microbiota indicate that interspecies interactions impact both the metabolism of a microbial community and the effect of antibiotics on individual species. For fly gut commensals, the pH-based mechanism underlying the tolerance of *Lp* induced by acetobacters is intrinsically connected to the metabolic capacity of each species, and hence is likely to be generally relevant *in vivo* to the resilience of this community under perturbations. Moreover, these findings could have important implications for human health, for example in the context of *Lactobacillus*-dominated vaginal microbiotas[25], and their generality should be tested broadly in other contexts.

In this study, we observed a novel form of antibiotic tolerance. Tolerance has been defined as increased time to killing[26], as opposed to resistance (a change in the MIC), or persistence (the ability of a subpopulation of clonal bacteria to survive high concentrations of antibiotic[5]). Tolerance to beta lactams such as ampicillin has been observed in *E. coli* cultures that exhibit slow growth or a long lag phase[5], and *E. coli* mutants with longer lag phases can be selected through experimental evolution to match the time of treatment[27,28]. Based on these previous studies, we were surprised to find the opposite effect with rifampin on *Lp*: cultures with a shorter lag phase exhibited increased tolerance (Fig. 1,4).

492 Moreover, although tolerance to erythromycin was associated with a longer lag
493 phase (Fig. 3e, 5a,h), killing retardation was at least an order of magnitude longer
494 than the change in lag time (Fig. 5a,h), indicating that tolerance is not determined
495 by an elongation of lag phase alone, in contrast to the effects of ampicillin on *E.*
496 *coli*[27].
497
498 Several genetic factors that increase time to killing have been identified in *E. coli*,
499 including toxin-antitoxin modules such as *hipBA*[29] that induce the stringent
500 response and thus cause transient growth arrest. In *Lp* co-culture with
501 acetobacters, metabolic interactions alter the physiological state of *Lp* during late
502 stationary phase by changing the environmental pH (Fig. 2). The stringent
503 response is required to survive acid shock in *Helicobacter pylori*[30] but not in
504 *Enterococcus faecalis*[31], which is in the same order as *Lp*. In the case of *Lp*, whether
505 the stringent response could be a major factor in the increased tolerance to
506 rifampin is unclear due to the surprising connection with decreased lag (not to
507 mention the opposite behavior with erythromycin).
508
509 The pH in stationary phase can affect many factors, such as the chemistry of
510 extracellular metabolites and macromolecules as well as the surface of the cell[32].
511 Importantly, our assays of antibiotic sensitivities were all performed at a starting

512 pH of 7. Nonetheless, shifts in extracellular pH can lead to buffered drops in
513 cytoplasmic pH[33,34]; such drops can be regulated[35] or result from internalization
514 of low-pK_a species such as short-chain fatty acids[36]. Such changes could lead to
515 protonation of macromolecules involved in adsorption or changes in the proton
516 motive force[37]. How these factors affect non-polycationic antibiotics such as
517 rifampin remains to be determined; neither of the ionizable functional groups of
518 rifampin (pK_as 1.7 and 7.9[38]) nor erythromycin (pK_a 8.88[39]) have pK_as in the pH
519 range achieved in our cultures (Fig. 2,S7b). Protonation changes in target
520 macromolecules could also lead to protection against antibiotics, although we
521 would expect a subsequent change in MIC, contrary to our findings (Fig. 1,5).
522 Intracellular acidification by the short-chain fatty acid propionate has been
523 proposed to lengthen lag phase in *Salmonella in vitro* and in the mouse gut[40],
524 consistent with our finding that lag time (Fig. 4) and intracellular pHluorin
525 fluorescence (Fig. S6a) are related.
526
527 Changes in intra- and extracellular pH have been shown to lead to
528 transcriptional responses that provide cross-protection against antibiotics[41-43],
529 suggesting that the killing retardation due to a pH increase in stationary phase
530 may result from a complex regulatory process. One major factor influencing the
531 *Lactobacillus-Acetobacter* interaction is that these organisms form a recurrent

532 community and may therefore have evolved to sense and benefit from each
533 other's presence. Further experiments are needed to uncover the molecular
534 mechanisms that link growth state and susceptibility to antibiotics in lactobacilli,
535 other non-model organisms, and microbial communities. In addition, although
536 we consistently observed related shifts in lag phase and tolerance (Fig. 3,5), it
537 remains to be established whether lag time and tolerance are causally linked or
538 coupled to some global variable, particularly given the opposite effects on
539 rifampin and erythromycin tolerance.
540
541 Previous work has shown that bacterial interactions can elicit changes in
542 antibiotic sensitivity by changing cellular physiology or interfering with
543 antibiotic action directly or indirectly[9-11]. In principle, a myriad of intra- and
544 extra-cellular variables are subject to the composition and dynamics of the
545 ecosystems that bacteria inhabit, and microbial communities within mammalian
546 hosts can elicit changes in environmental variables both locally and globally.
547 Specifically, the microaerobic and anaerobic microenvironments of the human
548 and fly[24] gastrointestinal tracts enable the growth of short chain fatty acid
549 producers. Some of these short chain fatty acids, like butyrate, have been shown
550 to play an important role on host physiology and health[44]. The consequences of
551 the accumulation of these short chain fatty acids and other small molecules on

552 microenvironments, as well as their effect on bacterial physiology and antibiotic
553 treatment efficacy *in vivo*, have yet to be systematically explored. Our results
554 emphasize the need to probe the action of antibiotics – as well as other drugs that
555 are thought not to target microbial growth[45] – in complex and varied conditions[46].
556 Furthermore, our findings highlight the utility of studying growth physiology in
557 co-cultures in the absence of antibiotics for uncovering novel mechanisms of
558 community-encoded protection against antibiotics.
559

Online Methods

Fruit fly stocks and gut microbiome sequencing

Wolbachia-free *Drosophila melanogaster* Canton-S (BL64349) flies were obtained from the Bloomington Drosophila Stock Center, and were reared and maintained as previously described[24]. To determine the bacterial strains present in our flies, we performed culture-independent 16S amplicon sequencing targeting the V4 region on an Illumina MiSeq. Individual flies were CO_2-anesthetized, surface-sterilized by washing with 70% ethanol and sterile PBS six times each. Flies were dissected under a stereo microscope and their guts were placed in 2-mL screw cap microtubes containing 200 µL of 0.1-mm sterile zirconia-silicate beads (BioSpec Products 11079101z) and 350 µL of sterile lysis buffer (10 mM Tris-HCl, pH 8, 25 mM NaCl, 1 mM EDTA, 20 mg/mL lysozyme). Samples were homogenized by bead beating at maximum speed (Mini-Beadbeater, BioSpec Products) for 1 min. Proteinase K was added at 400 µg/mL and samples were incubated for 1 h at 37 °C. Sample were then centrifuged (3,000 × *g* for 3 min) and 300 μL of the nucleic acids-containing supernatant were transferred to 1.7-mL microtubes. Genomic DNA from samples was cleaned up through a DNA Clean & Concentrator-5 column (Zymo Research D4014). Using the protocol described in Ref. [47] for library preparation and sequencing, we sequenced the gut contents

of 18 individual flies, three flies each from six independent vials. Paired-end 250-base pair sequencing generated >10,000 reads per sample. Reads were filtered using PrinSeq as in Ref [48]. The reads were then clustered into operational taxonomic units (OTUs) at 99% identity and assigned taxonomy using LOTUS[49] with the following parameters: [-threads 60 -refDB SLV -highmem 1 -id 0.99 -p miseq -useBestBlastHitOnly 1 -derepMin 3:10,10:3 -simBasedTaxo 1 -CL 3]. Redundant strain identities were collapsed into single OTUs. Common reagent contaminant strains were then removed[50]. After filtering, only five unique species were identified (Fig. 1a). We isolated these species in culture and verified the taxonomic identity of our isolates using Sanger sequencing of the complete 16S rRNA gene[13]. At 97% OTU clustering, only three species were found: *Acetobacter* sp., *Lactobacillus plantarum*, and *Lactobacillus brevis*. When less stringent FASTQ quality filtering was used, trace amounts (~0.01%) of two mammalian gut strains were identified: *Blautia* sp. and *Bacteroides* sp. Because these OTUs were eliminated by more stringent quality filtering, we speculate that they may have resulted from barcode bleed-through on the MiSeq flowcell.

Bacterial growth and media

Bacterial strains used in this study are listed in Supplementary Table 1. For culturing, all strains were grown in MRS medium (Difco™ Lactobacilli MRS

Broth, BD 288110). Frozen stocks were streaked onto MRS agar plates (1.5% agar, Difco™ agar, granulated, BD 214530) and single colonies were picked to start cultures. MYPL medium was adapted from Ref. [51], with 1% (w/v) D-mannitol (ACROS Organics AC125345000, Lot A0292699), 1% (w/v) yeast extract (Research Products International Y20020, Lot 30553), 0.5% (w/v) peptone (Bacto™ peptone, BD 211677 Lot 7065816), 1% (w/v) lactate (Lactic acid, Sigma L6661-100ML Lot MKCC6092), and 0.1% (v/v) Tween® 80 (Polyoxyethylene(20)sorbitan monooleate, ACROS Organics AC278632500 Lot A0375189). The medium was set to pH 7 with NaOH (EMD Millipore SX0590, Lot B0484969043). All media were filter-sterilized. Strains were grown at 30 °C with constant shaking.

To count CFUs in cultures, aliquots were diluted serially in PBS. For cultures treated with high concentrations of antibiotics, cells were centrifuged for 1.5 min at 8000 x *g* and resuspended in 1X PBS pH 7.4 (Gibco™ 70011044) after removing the supernatants. PBS-diluted cultures were plated on MRS and MYPL because lactobacilli grow faster than acetobacters on MRS and vice versa on MYPL. Colony morphology and color enable differentiation of lactobacilli from acetobacters.

Conditioned media

Conditioned media were obtained by centrifuging cultures at 4500 x *g* for 5 min and filtering the supernatant with a 0.22-μm polyethersulfone filter (Millex-GP SLGP033RS) to remove cells. Conditioned media were acidified with HCl (Fisher Chemical A144-500, Lot 166315) or basified with NaOH (EMD Millipore SX0590, Lot B0484969043). Conditioned media were sterilized after adjusting pH with 0.22-μm PES filters.

MIC estimations

To estimate the sensitivity of each species to various antibiotics, colonies were inoculated into MRS and grown for 48 h at 30 °C with constant shaking. Cultures were diluted to an OD of 0.001 for *Lp*, *Lb*, and *At*, and 0.01 for *Ap*. Diluted cultures (195 μL) were transferred to 96-well plates containing 5 μL of antibiotics at 40X the indicated concentration. Antibiotics used were ampicillin (ampicillin sodium salt, MP Biomedicals 02194526, Lot R25707, stock at 100 mg/mL in milliQ H_2O), streptomycin (streptomycin sulfate salt, Sigma S9137 Lot SLBN3225V, stock at 50 mg/mL in milliQ H_2O), chloramphenicol (Calbiochem 220551, Lot D00083225, stock at 50 mg/mL in ethanol), tetracycline (tetracycline hydrochloride, MP Biomedicals 02103011, Lot 2297K, stock at 25 mg/mL in dimethyl sulfoxide (DMSO)), erythromycin (Sigma E5389-1G, Lot WXBC4044V, stock at 64 mg/mL in methanol), ciprofloxacin (Sigma-Aldrich 17850, Lot

116M4062CV, stock at 1.2 mg/mL in DMSO), trimethoprim (Alfa Aesar J63053-03, Lot T16A009, stock at 2 mg/mL in DMSO), spectinomycin (spectinomycin hydrochloride, Sigma-Aldrich PHR1426-500MG, Lot LRAA9208, stock at 50 mg/mL in milliQ H_2O), rifampin (Sigma R3501-5G, Lot SLBP9440V, stock at 50 mg/mL in DMSO), and vancomycin (vancomycin hydrochloride, Sigma-Aldrich PHR1732-4X250MG, Lot LRAB3620, stock at 200 mg/mL in DMSO:H_2O 1:1). Antibiotics were diluted serially in 2-fold increments into MRS. Cultures were grown for 24 h at 30 °C with constant shaking and absorbance was measured in an Epoch2 plate reader (BioTek Instruments) at 600 nm. The MIC was estimated as the minimum concentration of antibiotic with absorbance within two standard deviations of media controls.

For experiments in Supplementary Figure S2, colonies of *Lp* and *Ap* were inoculated into MRS and grown for 48 h at 30 °C with constant shaking. The saturated cultures were diluted to OD 0.02, mixed 1:1, and grown for 48 h at 30 °C with constant shaking. Then, the mono- and co-cultures were diluted to an OD of 0.001 (final cell density ~5×10^5 CFU/mL) and transferred to 96-well plates containing 5 μL of rifampin at 40X working concentration. Cultures were grown for 24 h and MICs were estimated as described above. For Figures 1b-e, cultures were serially diluted in 5-fold increments in PBS, and 3 μL of the dilutions were

660 spotted onto MRS and MYPL rectangular plates using a semi-automated high-
661 throughput pipetting system (BenchSmart 96, Mettler Toledo). Plates were
662 incubated at 30 °C until colonies were visible for quantification of viability.
663
664 *Plate reader growth curves*
665 Cultures were grown from single colonies for 48 h in MRS at 30 °C with constant
666 shaking. Then, cultures were diluted to a final OD of 0.02 and 200 μL of the
667 dilutions were transferred to clear-bottom transparent 96-well plates. Plates were
668 sealed with transparent film pierced with a laser cutter to have ~0.5-mm holes to
669 allow aeration in each well. Absorbance was measured at 600 nm in an Epoch2
670 plate reader (BioTek Instruments). Plates were shaken between readings with
671 linear and orbital modes for 145 s each.
672
673 Growth rates and lag times were quantified using custom MATLAB (Mathworks,
674 R2008a) code. The natural logarithm of OD was smoothed with a mean filter
675 with window size of 5 timepoints for each condition over time, and the smoothed
676 data were used to calculate the instantaneous growth rate $d(\ln(OD))/dt$. The
677 smoothed ln(OD) curve was fit to the Gompertz equation[52] to determine lag time
678 and maximum growth rate.
679

680 *pH measurements*

681 Culture pH was measured using the dual-excitation ratiometric pH indicator
682 2',7-bis-(2-carboxyethyl)-5-(and-6)-carboxyfluorescein, mixed isomers (BCECF,
683 Invitrogen B1151, Lot 1831845), which has a pK_a of ~6.98. A stock solution of 1
684 mg/mL BCECF in DMSO (Fisher BioReagents BP231, Lot 165487) was diluted
685 1000-fold into MRS to a final concentration of 1 μg/mL. Cells were grown in a
686 Synergy H1 plate reader (BioTek Instruments) following the procedure described
687 above. In addition to absorbance, fluorescence was measured every cycle using
688 monochromators at excitation (nm)/emission (nm) wavelength combinations
689 440/535 and 490/535. After subtracting the fluorescence of wells containing cells
690 without the indicator, the ratio of the signals excited at 440 nm and 490 nm was
691 used to calculate the culture pH using a calibration curve of MRS set to various
692 pH values.

693

694 Culture pH after 48 h of growth was directly measured with a pH meter
695 (sympHony, VWR) equipped with a pH combination electrode (Fisherbrand™
696 accumet™ 13-610-104A).

697

698 *Changes in pH during growth*

To change the pH of monocultures and co-cultures in stationary phase, we obtained conditioned medium at 30 h or 40 h as described above and set the pH to the desired values. We then centrifuged 2 mL of a replicate culture for 3 min at 8000 x *g*, removed the supernatant, and resuspended cells in 1 mL of the corresponding medium to wash the cells. The suspension was centrifuged a second time and the pellets were resuspended in 2 mL of the corresponding medium.

Time-lapse and fluorescence microscopy

Cells were imaged on a Nikon Eclipse Ti-E inverted fluorescence microscope with a 100× (NA 1.40) oil-immersion objective. Images were collected on a DU897 electron multiplying charged couple device camera (Andor) using μManager v. 1.4[53]. Cells were maintained at 30 °C during imaging with an active-control environmental chamber (Haison).

Cultures grown for 48 h were diluted 100-fold into PBS and 2 μL were spotted onto a 1% (w/v) agarose MRS pad. After drying at room temperature, the pads were covered with a cover slip, sealed with a mixture of equal portions of Vaseline, lanolin, and paraffin, and transferred to the microscope. Images were taken every 2 min using μManager v. 1.4.

719

720 To quantify the morphology of cells using fluorescent strains, co-cultures were
721 diluted 100-fold into PBS and 2 μL were spotted onto a 1% (w/v) agarose PBS
722 pad. After drying, the pads were covered with a cover slip and transferred to the
723 microscope. Images were acquired at room temperature using μManager v. 1.4.

724

725 For Figure S6, saturated *Ap* monocultures were diluted 100- or 500-fold into PBS
726 and 2 μL were spotted onto a 1% (w/v) agarose MRS pad containing 30 μM
727 propidium iodide (from a 4.3-mM stock in water, BD, Cell Viability Kit 349483).
728 After drying, the pads were covered with a cover slip and transferred to the
729 microscope. Images were taken at 30 °C every 5 min using μManager v. 1.4.

730

731 The MATLAB image processing software *Morphometrics*[54] was used to segment
732 cells and to identify cell contours from phase-contrast images. Fluorescence
733 intensity per cell was calculated by averaging the fluorescence over the area of
734 the cell. A threshold for propidium-iodide labeling was defined that clearly
735 separated labeled cells from unlabeled cells (data not shown).

736

737 *Single-cell tracking and analysis*

738 Images were segmented and cells were tracked using the software *SuperSegger* v.
739 3[55]. Further analysis of single-cell growth was performed using custom MATLAB
740 code. Cells with length >6 μm were removed from further analysis due to issues
741 with segmentation. Length traces were smoothed using a mean filter of window
742 size 5. Cells were classified as *Lp* or *Ap* if 90% of their traces were above (*Lp*) or
743 below (*Ap*) a $\log_{10}$(length-to-width ratio) of 0.375. Traces with more than 15
744 timepoints were used for further analysis. Elongation rates $d(\ln L)/dt$ were
745 calculated for each cell and the mean and standard error were computed for each
746 time point.
747
748 *Cloning and transformations*
749 To generate the fluorescently labeled *Ap* strain, the sfGFP coding sequence was
750 cloned into pCM62[56] under control of the *Escherichia coli* lac promoter. The sfGFP
751 coding sequence was amplified from pBAD-sfGFP using primers ZTG109 (5′
752 ggatttatgcATGAGCAAGGGCGAGGAG) and ZTG110 (5′-
753 gctttgttagcagccggatcgggcccggatctcgagTTACTTGTACAGCTCGTCCATG).
754 Gibson assembly[57] was used to insert the amplified sfGFP cassette into
755 BglII/XhoI-digested pCM62. This construct was delivered into *Ap* by conjugation
756 as previously described[58]. *Escherichia coli* BW29427 was used as a donor strain
757 and maintained with 80 mg/mL 2,6-Diaminopimelic acid (Sigma Aldrich

33240)in potato agar mating plates[58]. Transformed *Ap* was selected with 10 μg/mL tetracycline on yeast peptone glycerol agar plates[58].

To generate the *Lp* strain harboring pHluorin, the pHluorin coding sequence was cloned into pCD256-mCherry[59] under the control of the strong p11 promoter[20]. The pHluorin coding sequence was amplified using primers ZFH064-pHluorin (5'-ATTACAAGGAGATTTTACAT ATGAGTAAAGGAGAAGAACTTTTC) and ZFH065-pHluorin (5'-gtctcggacagcggttttGGATCCTTATTTGTATAGTTCATCCATG). Gibson assembly[57] was used to insert the amplified pHluorin cassette into NdeI/BamHI-digested pCD256-mCherry. The *Lp*-pHluorin strain was generated by transforming wild type *Lp* as previously described[60].

Fluorescent strains were further grown in MRS with antibiotics (10 μg/mL chloramphenicol (Calbiochem 220551, Lot D00083225) for *Lp*, tetracycline (10 μg/mL tetracycline hydrochloride, MP Biomedicals 02103011, Lot 2297K) for *Ap*).

pHluorin measurements

Cells were grown following the procedure described above. The *Lp* pHluorin strain was grown in MRS containing 10 μg/mL chloramphenicol for the first 48 h

of growth. In addition to absorbance, fluorescence was measured every cycle using monochromators at excitation (nm)/emission (nm) wavelength combinations 405/509 and 475/509. Because the signal from excitation wavelength 405 nm was undistinguishable from signal from medium (data not shown), we also measured pHluorin signal at both excitation/emission wavelength combinations for cells in PBS. Cultures (48-h-old, 250 μL) were centrifuged at 10,000 x *g* for 1 min and resuspended in 1X PBS. Aliquots (200 μL) were transferred to a 96-well plate and fluorescence was measured using monochromators at excitation (nm)/emission (nm) wavelength combinations 405/509 and 475/509 within 1 min of resuspension in a Synergy H1 plate reader (BioTek Instruments).

Lactate measurements

Colonies of *Lp* and acetobacters were inoculated into 3 mL MRS and grown for 48 h at 30 °C with constant shaking. Saturated cultures were diluted to OD 0.02, mixed 1:1, and grown at 30 °C with constant shaking. After mixing for 20 h and 48 h, a 700-μL aliquot was transferred to a microcentrifuge tube and centrifuged at 10,000 x *g* for 4 min. Supernatant (600 μL) was transferred to a new tube and centrifuged at 10,000 x *g* for 4 min. Supernatant (500 μL) was transferred to a new tube and kept on ice for not longer than 1 h, until lactate was measured.

798

799 L- and D-lactate concentrations were measured using the EnzyChrom™ L-
800 (BioAssay Systems ECLC-100, Lots BH06A30 and BI07A09) and D-lactate
801 (BioAssay Systems EDLC-100, Lots BH0420 and BI09A07) Assay Kits. Samples
802 were diluted 10- and 100-fold in water, and absorbance was measured according
803 to the manufacturer's instructions in a plate reader (Tecan M200). We also
804 included controls without lactate dehydrogenase to account for endogenous
805 activity in the supernatants.

806

807 Ex vivo *experiments*

808 We generated germ-free flies by sterilizing dechorionated embryos. Embryos
809 oviposited on grape juice-yeast medium (20% organic grape juice, 10% active dry
810 yeast, 5% glucose, 3% agar) were harvested and washed twice with 0.6% sodium
811 hypochlorite for 2.5 min each, once with 70% ethanol for 30 s, and three times in
812 sterile water for 10 s each. Eggs were transferred into flasks with sterile glucose-
813 yeast medium (10% glucose, 5% active dry yeast, 1.2% agar, 0.42% propionic
814 acid) and were maintained at 25 °C with 60% humidity and 12 h light/dark
815 cycles. Germ-free stocks of these flies were kept for several generations and were
816 regularly checked for sterility by plating flies onto MRS and YPD media.

817

To prepare flies for tolerance measurements, we took ~3-day-old germ-free flies and transferred them to sterile vials with ~50 flies each. We added ~5 x 10^6 CFU of *Lp* onto the food and let the flies equilibrate with the bacteria for 3 days. The day before the experiment, flies were transferred into a clean sterile vial.

To extract the midgut and crop, flies were washed with 70% ethanol and PBS six times each. Flies were dissected under a stereo microscope in sterile PBS. Dissected crops and midguts were pooled into 2 mL of sterile MRS with 200 μL 0.5-mm diameter sterile zirconia-silicate beads (BioSpec Products 11079105). Suspended organs were homogenized in a bead beater (Mini-Beadbeater, BioSpec Products) at maximum speed for 1 min. The homogenate was diluted to a cell density of ~5 x 10^5 CFU/mL and was treated with 50 μg/mL rifampin for 24 h.

Statistical analyses

To determine significance of differences, we performed pairwise Student's two-sided *t*-tests throughout. To decrease Type I error, we performed Bonferroni corrections for each experiment. Significant differences are denoted in the figures: *: $P<0.05/n$, **: $P<0.01/n$, ***: $P<0.001/n$, where n is the number of comparisons.

Acknowledgments

The authors thank Vivian Zhang for technical support, Elizabeth Skovran for kindly providing the pCM62 plasmid for *Acetobacter* spp., and Kazunobu Matsushita for providing the *A. tropicalis* SKU1100 control strain in the initial conjugation experiments. We also thank the Huang and Ludington labs for fruitful discussions. This work was supported by NIH Director's New Innovator Awards DP2OD006466 (to K.C.H.), NSF CAREER Award MCB-1149328 (to K.C.H.), the Allen Center for Systems Modeling of Infection (to K.C.H.), and NIH Director's Early Independence Award DP5OD017851 (to W.B.L.). K.C.H. is a Chan Zuckerberg Biohub Investigator. A.A.-D. is a Howard Hughes Medical Institute International Student Research fellow and a Stanford Bio-X Bowes fellow.

Author Contributions

A.A.-D., K.C.H., and W.B.L designed the research. A.A.-D. and T.T. performed *in vitro* experiments. A.A.-D. and B.O. performed *ex vivo* experiments. B.O., Z.T.G., and Z.H. built fluorescent strains. A.A.-D. analyzed the data. A.A.-D., K.C.H., and W.B.L. wrote the paper. All authors reviewed the paper before submission.

Figure Legends

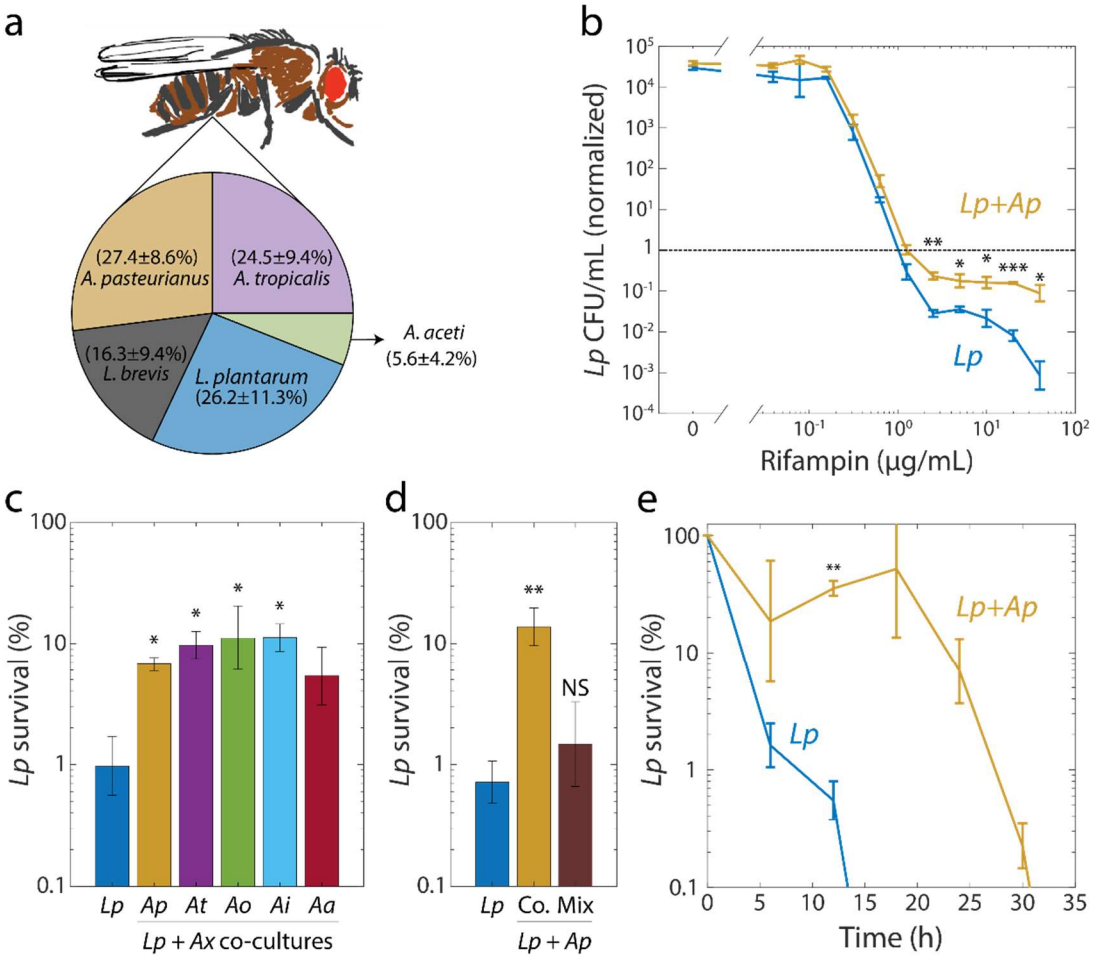

Figure 1: Interspecies interactions within the fruit fly gut microbiome induce rifampin tolerance.

a) Relative abundances of the dominant species in the *D. melanogaster* gut microbiome determined from 16S rRNA sequencing. Values are mean ± standard deviation (S.D.), *n*=18. Mean and S.D. were weighed by the total number of reads for each fly.

b) When grown with *Ap*, *Lp* survived after 24 h at rifampin concentrations above the MIC. Viable cell plating counts of *Lp* after growth in rifampin for 24 h normalized to the counts at the start of the experiment (t=0). Error bars are standard deviation (S.D.) for each condition, n=3. P-values are from a Student's two-sided t-test of the difference of the co-culture from the monoculture (*: $P<4\times10^{-3}$, **: $P<8\times10^{-3}$, ***: $P<8\times10^{-5}$).

c) Protection of *Lp* at supra-MIC concentrations of rifampin is elicited by all acetobacters tested. Normalized CFUs of *Lp* grown in monoculture (*Lp*) or in co-culture with *Ap*, *At*, *Ao*, *Ai*, and *Aa*, and then treated with 20 μg/mL rifampin for 24 h. Error bars are S.D. for each condition, n=3. P-values are from a Student's two-sided t-test of the difference from the monoculture (*: $P<0.01$).

d) *Ap*-mediated survival of *Lp* at rifampin concentrations above the MIC is history-dependent, requiring co-culturing before exposure as compared with mixing. Normalized CFUs of *Lp* grown in monoculture, in co-culture with *Ap* (Co.), or mixed with *Ap* without subsequent growth in the absence of antibiotic (mix), and treated with 20 μg/mL rifampin for 24 h. Error bars are S.D. for each condition, n=3. P-values are from a Student's two-sided t-test of the difference from the monoculture (**: $P<5\times10^{-3}$, NS: not significant).

e) The time to killing of *Lp* under rifampin treatment is extended in the presence of an *Acetobacter*. Normalized CFUs of *Lp* grown in monoculture and co-cultured with *Ap*, and treated with 50 μg/mL rifampin. Error bars are S.D. for each condition, n=3. P-values are from a Student's two-sided t-test of the difference from the monoculture at the corresponding timepoint (**: $P<1x10^{-3}$). Values off the graph were below the limit of detection of the assay

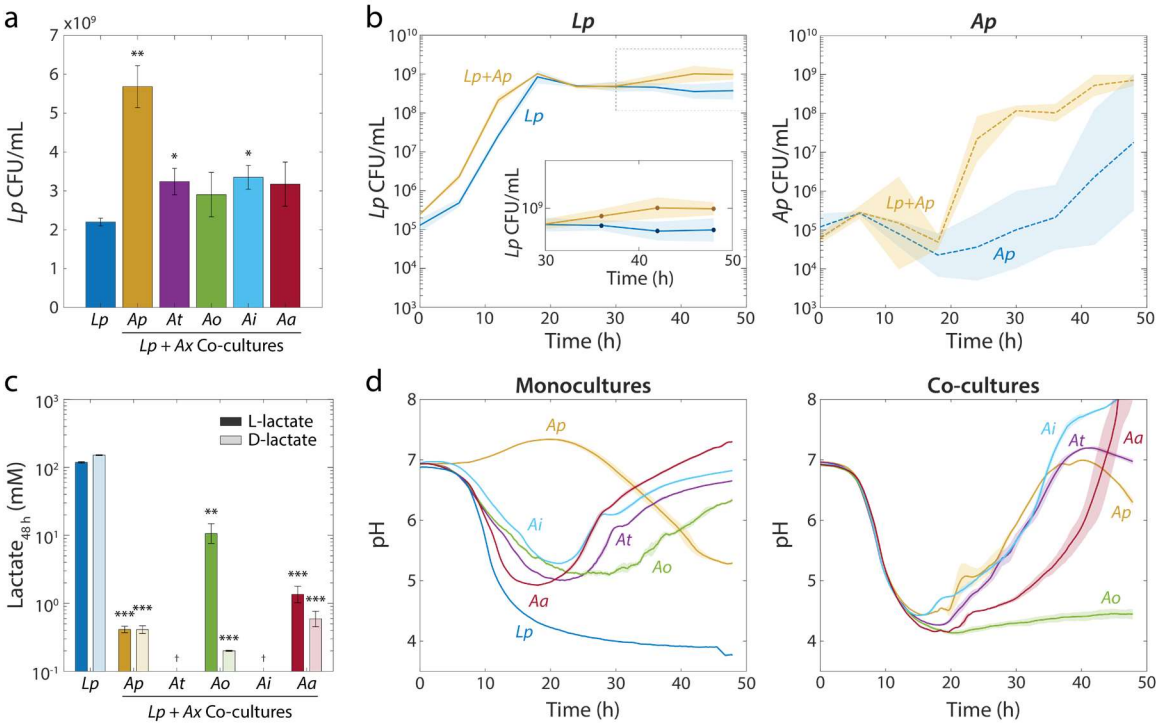

Figure 2: *Lp* growth during stationary phase in *Acetobacter* co-cultures is associated with an increase in pH and a decrease in lactate concentration.

a) Co-culturing *Lp* with *Ap*, *At*, *Ai*, or *Aa* resulted in increased *Lp* cell density after 48 h. Co-culturing with *Ao* did not significantly increase *Lp* cell density by 48 h. Error bars are standard deviation (S.D.) for each condition, n=3. P-values are from a Student's two-sided t-test of the difference from the monoculture (*: P<0.01, **: P<2x10^{-3}).

b) Co-culturing *Lp* with *Ap* resulted in higher *Lp* cell density in stationary phase, as well as faster growth and shorter lag for *Ap*. Shaded regions indicate S.D., n=3. Inset: zoom-in on region inside dashed box highlighting increase in carrying capacity in co-culture.

c) L- and D-lactate were produced in *Lp* monocultures and consumed in co-cultures. Lactate concentration was measured enzymatically from culture supernatants at 48 h. Error bars are S.D. for each condition, n=3. P-values are from a Student's two-sided t-test of the difference from the monoculture (**: $P<2\times10^{-3}$, ***: $P<2\times10^{-4}$).

d) The increase in *Lp* cell density in stationary phase is associated with an *Acetobacter*-dependent increase in pH early in stationary phase. pH was measured with the pH-sensitive dye 2',7-bis-(2-carboxyethyl)-5-(and-6)-carboxyfluorescein over time (Methods). Shaded regions indicate S.D., n=3.

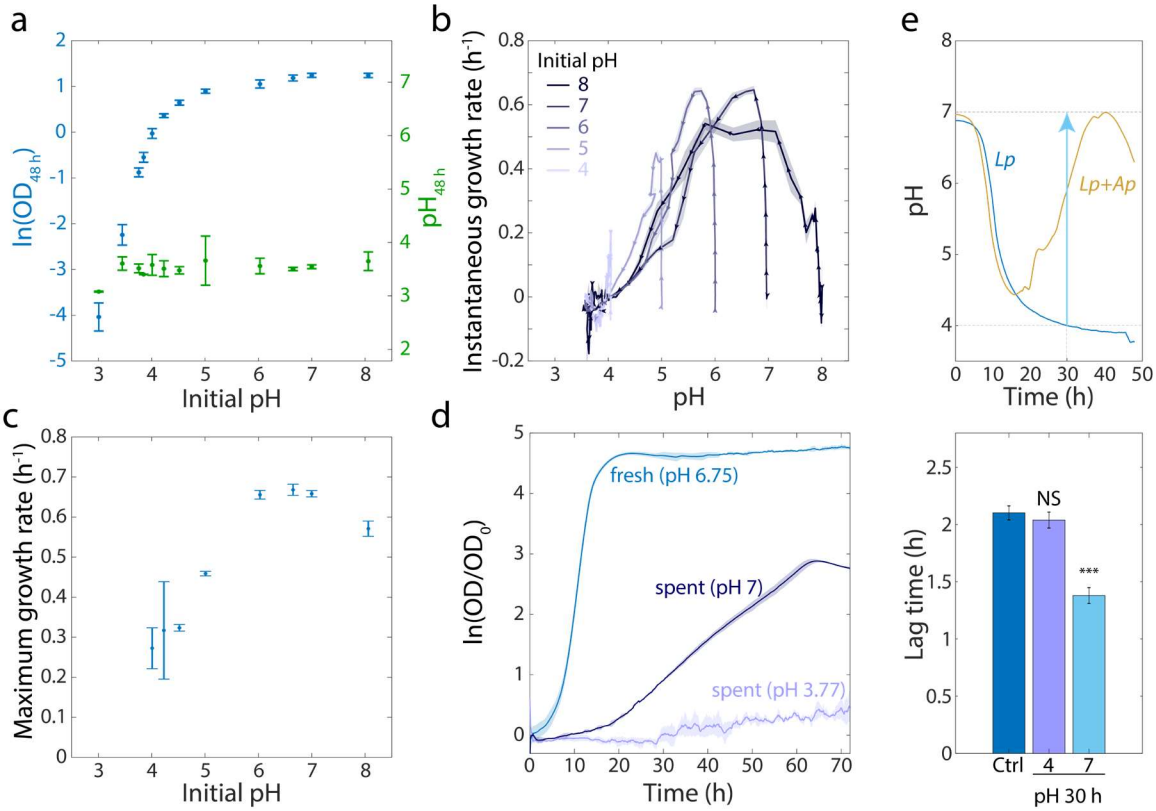

Figure 3: An increase in extracellular pH in stationary phase releases growth inhibition in *Lp* monocultures and shortens lag phase.

a) *Lp* growth is inhibited by low pH. Logarithm of OD (blue) and pH measured using BCECF (green) after 48 h of growth in MRS at various starting pH values. Error bars are standard deviation (S.D.), n=4.

b) Instantaneous growth rate in MRS is strongly linked to pH. Each curve was initialized at a different starting pH and represents 48 h of growth. Arrowheads indicate direction of time. Shaded regions are S.D., n=4.

c) Maximal growth rate in MRS increases with increasing initial pH. Error bars are S.D., n=4.

d) Increasing the pH of a saturated, spent *Lp* culture from 3.77 to 7 allows growth, although not as much as fresh MRS. Error bars are S.D., $n = 3$.

e) Increasing the pH of an *Lp* monoculture at $t = 30$ h from 4 to 7 to mimic the pH increase in *Lp-Ap* co-culture (top) leads to a shorter lag phase (bottom). Lag time was calculated by fitting growth curves to the Gompertz equation. Error bars are S.D., n=3. *P*-values are from a Student's two-sided *t*-test of the difference from the control (***: $P<5\text{x}10^{-4}$, NS: not significant).

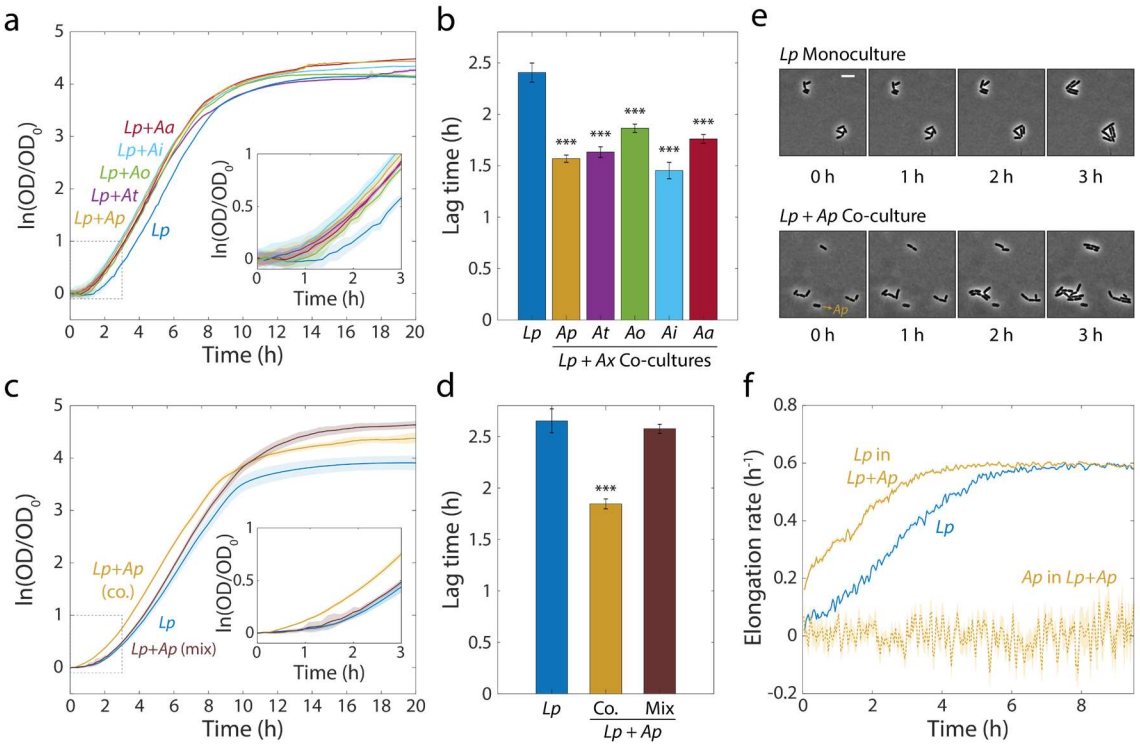

Figure 4: Co-cultures of *Lp* and acetobacters undergo shorter lag phases.

a) Calculating the logarithm of OD normalized by OD at t=0 reveals that co-cultures of *Lp* and various acetobacters (*Ax*) experience more rapid transitions from stationary phase to exponential growth than monocultures of *Lp*. Shaded regions indicate standard deviation (S.D.), n=5. Inset: zoom-in of region inside dashed box highlighting lag differences.

b) Co-culture lag times are significantly shorter than *Lp* monoculture lag times. Lag times were obtained by fitting the growth curves in (a) to the Gompertz equation. Error bars are S.D. for each condition, n=5. P-values

942 are from a Student's two-sided *t*-test of the difference from the
943 monoculture (***: $P<2x10^{-4}$).
944 c) Mixing *Lp* monocultures with *Ap* monocultures (Mix) yields growth
945 curves with a similar lag phase than those of *Lp* monocultures. Shaded
946 regions indicate S.D., *n*=5. Inset: zoom-in on region inside dashed box
947 highlighting lag differences.
948 d) Mixed *Lp*-*Ap* cultures do not experience significantly shorter lag times
949 than *Lp* monocultures. Lag times were obtained by fitting the curves in (c)
950 to the Gompertz equation. Error bars are S.D. for each condition, *n*=5. *P*-
951 values are from a Student's two-sided *t*-test of the difference from the
952 monoculture (***: $P<5x10^{-4}$).
953 e) Single-cell microscopy demonstrates that a decrease in the duration of lag
954 phase of *Lp* was responsible for the lag-time decrease in co-culture.
955 Representative phase microscopy images of *Lp* in monoculture and co-
956 cultured with *Ap* on an MRS agar pad. The only *Ap* cell visible in these
957 images is indicated with an arrow. Size bar = 5 μm.
958 **f)** The instantaneous elongation rate of single *Lp* cells increases faster in co-
959 culture than in monoculture. Phase-contrast images were segmented and
960 cells were classified as *Lp* or *Ap* based on their aspect ratio. Lines are the
961 mean and shaded regions are the standard error for an *Lp* monoculture

962 ($n_{Lp,0\,h}$ = 465, $n_{Lp,9.5\,h}$ = 27,503) or a co-culture with *Ap* ($n_{Lp,0\,h}$ = 448, $n_{Lp,9.5\,h}$ =

963 58,087, $n_{Ap,0\,h}$ = 47, $n_{Ap,9.5\,h}$ = 146).

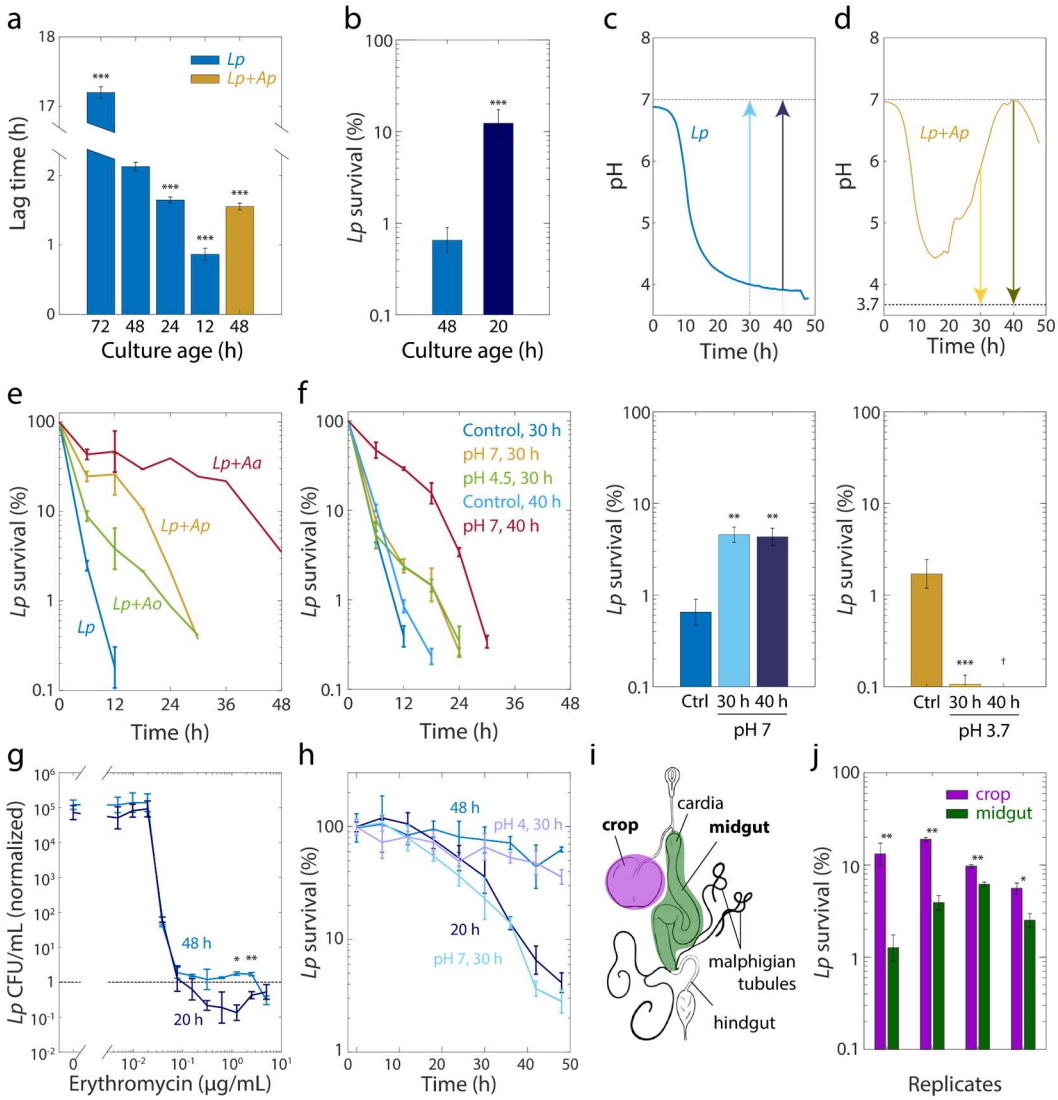

Figure 5: Tolerance to rifampin is modulated by pH.

a) The duration of lag phase of bulk cultures of *Lp* depends on the time spent in stationary phase. *Lp* monocultures grown for various times from OD=0.02, and co-cultures with *Ap*, were diluted into fresh medium. Lag time was calculated by fitting growth curves to the Gompertz equation. Error bars are standard deviation (S.D.), n=12. P-values are from a

971 Student's two-sided *t*-test of the difference with respect to the 48 h culture
972 (***$P<2.5x10^{4}$).

973 b) Culturing *Lp* as a monoculture for a shorter time leads to higher cell
974 survival. Viable cell plating counts of *Lp* after growth in 20 μg/mL
975 rifampin for 24 h normalized to the counts at the start of the experiment
976 (*t*=0). Error bars are S.D. for each condition, *n*=3. *P*-values are from a
977 Student's two-sided *t*-test of the difference between the cultures (***:
978 $P<1x10^{-3}$).

979 c) Neutralization of pH in stationary phase in *Lp* monocultures is sufficient
980 to induce tolerance. Increasing the pH of an *Lp* monoculture at *t* = 30 h or *t*
981 = 40 h to 7 to mimic the pH increase in co-cultures of *Lp* with acetobacters
982 (upper panel) increased cell survival after treatment with 20 μg/mL
983 rifampin for 24 h (lower panel). A 48-h-old culture with no changes in pH
984 was used as a control (Ctrl.). Error bars are S.D. for each condition, *n*=3. *P*-
985 values are from a Student's two-sided *t*-test of the difference between the
986 cultures (**: $P<5x10^{-3}$).

987 d) Acidification of *Lp* co-cultures with *Ap* during the exponential-to-
988 stationary phase transition or in late stationary phase sensitizes *Lp* to
989 rifampin. Decreasing the pH of an *Lp* co-culture with *Ap* at *t* = 30 h or *t* =
990 40 h to 3.7 to mimic the pH of an *Lp* monoculture (upper panel) increased

survival after treatment with 20 μg/mL rifampin for 24 h (lower panel). Error bars are S.D. for each condition, *n*=3. *P*-values are from a Student's two-sided *t*-test of the difference between the cultures (***: $P<5x10^{-4}$). †Values below the limit of detection.

e) The dynamics of killing in *Lp* co-culture with acetobacters differs quantitatively according to species and from *Lp* monoculture (blue), indicating that the acetobacters induce rifampin tolerance to different degrees. Normalized CFU/mL of *Lp* in monoculture and in co-culture with acetobacters, and treated with 50 μg/mL rifampin. Error bars are S.D. for each condition, *n*=3.

f) The timing of the pH change in *Acetobacter* co-culture predicts the extent of protection against 50 μg/mL rifampin. Neutralization of pH in *Lp* monocultures at 40 h of growth (to mimic *Lp*+*Aa* co-cultures) elicits longer protection against rifampin than neutralization at 30 h. A small increase in pH (from 3.85 to 4.5) at 30 h (to mimic *Lp*+*Ao* co-cultures) provides protection comparable to complete neutralization. Error bars are S.D. for each condition, *n*=3.

g) *Lp* survival to erythromycin is ~10 times higher after 24 h of treatment with erythromycin at supraMIC concentrations on 48-h-old monocultures (48 h) of *Lp* than on 20-h-old *Lp* monocultures (20 h). Viable cell plating

1011 counts of *Lp* after growth in erythromycin for 24 h normalized to cell
1012 counts at the start of the experiment (*t*=0). Error bars are S.D., *n* = 3. *P*-
1013 values are from a Student's two-sided *t*-test of the difference between the
1014 two samples at a given time point (*: $P<4x10^{-3}$, **: $P<8x10^{-4}$).

1015 h) Shifting the pH of an *Lp* monoculture at 30 h to 4 or 7, followed by 18 h of
1016 growth before treatment with 2 μg/mL erythromycin, mimics the survival
1017 dynamics of a 48-h-old or 20-h-old culture in stationary phase,
1018 respectively. Normalized CFU/mL of *Lp* monocultures. Error bars are S.D.
1019 for each condition, *n*=3.

1020 i) Schematic of the fruit fly intestinal tract, a ~5 mm-long tube consisting of
1021 the foregut, midgut, and hindgut. The crop is an accessory fermentative
1022 organ within the foregut.

1023 j) Survival of *Lp* is significantly higher in bulk cultures resuspended from
1024 the crop than in cultures resuspended from the midgut. Female, ~7-day-
1025 old, germ-free flies were colonized with *Lp* and left for three days in sterile
1026 food to reach equilibrium, before the crop was dissected from the midgut
1027 (Methods). After homogenization of pools of crops and midguts, the
1028 cultures were exposed to 50 μg/mL rifampin for 24 h and viable cells were
1029 counted via CFU. Error bars are S.D. of the technical replicates for each
1030 biological replicate, *n*=3 in each biological replicate. *P*-values are from a

1031 Student's two-sided *t*-test of the difference between the two samples (*:

1032 $P<1.25\text{x}10^{-2}$, **: $P<2.5\text{x}10^{-3}$).

References

1 Thulin, E., Sundqvist, M. & Andersson, D. I. Amdinocillin (Mecillinam) resistance mutations in clinical isolates and laboratory-selected mutants of Escherichia coli. *Antimicrob Agents Chemother* **59**, 1718-1727, doi:10.1128/AAC.04819-14 (2015).

2 Dethlefsen, L., Huse, S., Sogin, M. L. & Relman, D. A. The pervasive effects of an antibiotic on the human gut microbiota, as revealed by deep 16S rRNA sequencing. *PLoS Biol* **6**, e280, doi:10.1371/journal.pbio.0060280 (2008).

3 Jernberg, C., Lofmark, S., Edlund, C. & Jansson, J. K. Long-term ecological impacts of antibiotic administration on the human intestinal microbiota. *ISME J* **1**, 56-66, doi:10.1038/ismej.2007.3 (2007).

4 Santajit, S. & Indrawattana, N. Mechanisms of Antimicrobial Resistance in ESKAPE Pathogens. *Biomed Res Int* **2016**, 2475067, doi:10.1155/2016/2475067 (2016).

5 Brauner, A., Fridman, O., Gefen, O. & Balaban, N. Q. Distinguishing between resistance, tolerance and persistence to antibiotic treatment. *Nat Rev Microbiol* **14**, 320-330, doi:10.1038/nrmicro.2016.34 (2016).

6 Nicoloff, H. & Andersson, D. I. Indirect resistance to several classes of antibiotics in cocultures with resistant bacteria expressing antibiotic-modifying or -degrading enzymes. *J Antimicrob Chemother* **71**, 100-110, doi:10.1093/jac/dkv312 (2016).

7 Sanchez-Vizuete, P., Orgaz, B., Aymerich, S., Le Coq, D. & Briandet, R. Pathogens protection against the action of disinfectants in multispecies biofilms. *Front Microbiol* **6**, 705, doi:10.3389/fmicb.2015.00705 (2015).

8 de Vos, M. G. J., Zagorski, M., McNally, A. & Bollenbach, T. Interaction networks, ecological stability, and collective antibiotic tolerance in polymicrobial infections. *Proc Natl Acad Sci U S A* **114**, 10666-10671, doi:10.1073/pnas.1713372114 (2017).

9 Adamowicz, E. M., Flynn, J., Hunter, R. C. & Harcombe, W. R. Cross-feeding modulates antibiotic tolerance in bacterial communities. *ISME J*, doi:10.1038/s41396-018-0212-z (2018).

10 Radlinski, L. *et al.* Pseudomonas aeruginosa exoproducts determine antibiotic efficacy against Staphylococcus aureus. *PLoS Biol* **15**, e2003981, doi:10.1371/journal.pbio.2003981 (2017).

11 Sorg, R. A. *et al.* Collective Resistance in Microbial Communities by Intracellular Antibiotic Deactivation. *PLoS Biol* **14**, e2000631, doi:10.1371/journal.pbio.2000631 (2016).

12 Ratzke, C. & Gore, J. Modifying and reacting to the environmental pH can drive bacterial interactions. *PLoS Biol* **16**, e2004248, doi:10.1371/journal.pbio.2004248 (2018).

13 Gould, A. L. *et al.* Microbiome interactions shape host fitness. *Proc Natl Acad Sci U S A*, doi:10.1073/pnas.1809349115 (2018).

14 Wong, C. N., Ng, P. & Douglas, A. E. Low-diversity bacterial community in the gut of the fruitfly Drosophila melanogaster. *Environ Microbiol* **13**, 1889-1900, doi:10.1111/j.1462-2920.2011.02511.x (2011).

15 Makarova, K. *et al.* Comparative genomics of the lactic acid bacteria. *Proc Natl Acad Sci U S A* **103**, 15611-15616, doi:10.1073/pnas.0607117103 (2006).

16 Yamada, Y., Hoshino, K. & Ishikawa, T. The phylogeny of acetic acid bacteria based on the partial sequences of 16S ribosomal RNA: the elevation of the subgenus Gluconoacetobacter to the generic level. *Biosci Biotechnol Biochem* **61**, 1244-1251, doi:10.1271/bbb.61.1244 (1997).

17 Walsh, C. & Wencewicz, T. A. *Antibiotics : challenges, mechanisms, opportunities*. (ASM Press, 2016).

18 James-Kracke, M. R. Quick and accurate method to convert BCECF fluorescence to pHi: calibration in three different types of cell preparations. *J Cell Physiol* **151**, 596-603, doi:10.1002/jcp.1041510320 (1992).

19 Martinez, K. A., 2nd *et al.* Cytoplasmic pH response to acid stress in individual cells of Escherichia coli and Bacillus subtilis observed by fluorescence ratio imaging microscopy. *Applied and environmental microbiology* **78**, 3706-3714, doi:10.1128/AEM.00354-12 (2012).

20 Rud, I., Jensen, P. R., Naterstad, K. & Axelsson, L. A synthetic promoter library for constitutive gene expression in Lactobacillus plantarum. *Microbiology* **152**, 1011-1019, doi:10.1099/mic.0.28599-0 (2006).

21 Levin-Reisman, I. *et al.* Automated imaging with ScanLag reveals previously undetectable bacterial growth phenotypes. *Nat Methods* **7**, 737-739, doi:10.1038/nmeth.1485 (2010).

22 Buchon, N. *et al.* Morphological and molecular characterization of adult midgut compartmentalization in Drosophila. *Cell Rep* **3**, 1725-1738, doi:10.1016/j.celrep.2013.04.001 (2013).

23 Strand, M. & Micchelli, C. A. Quiescent gastric stem cells maintain the adult Drosophila stomach. *Proc Natl Acad Sci U S A* **108**, 17696-17701, doi:10.1073/pnas.1109794108 (2011).

24 Obadia, B. *et al.* Probabilistic Invasion Underlies Natural Gut Microbiome Stability. *Curr Biol* **27**, 1999-2006 e1998, doi:10.1016/j.cub.2017.05.034 (2017).

25 Boris, S. & Barbes, C. Role played by lactobacilli in controlling the population of vaginal pathogens. *Microbes Infect* **2**, 543-546 (2000).

26 Brauner, A., Shoresh, N., Fridman, O. & Balaban, N. Q. An Experimental Framework for Quantifying Bacterial Tolerance. *Biophys J* **112**, 2664-2671, doi:10.1016/j.bpj.2017.05.014 (2017).

27 Fridman, O., Goldberg, A., Ronin, I., Shoresh, N. & Balaban, N. Q. Optimization of lag time underlies antibiotic tolerance in evolved bacterial populations. *Nature* **513**, 418-421, doi:10.1038/nature13469 (2014).

28 Levin-Reisman, I. *et al.* Antibiotic tolerance facilitates the evolution of resistance. *Science* **355**, 826-830, doi:10.1126/science.aaj2191 (2017).

29 Rotem, E. *et al.* Regulation of phenotypic variability by a threshold-based mechanism underlies bacterial persistence. *Proc Natl Acad Sci U S A* **107**, 12541-12546, doi:10.1073/pnas.1004333107 (2010).

30 Mouery, K., Rader, B. A., Gaynor, E. C. & Guillemin, K. The stringent response is required for Helicobacter pylori survival of stationary phase, exposure to acid, and aerobic shock. *J Bacteriol* **188**, 5494-5500, doi:10.1128/JB.00366-06 (2006).

31 Abranches, J. *et al.* The molecular alarmone (p)ppGpp mediates stress responses, vancomycin tolerance, and virulence in Enterococcus faecalis. *J Bacteriol* **191**, 2248-2256, doi:10.1128/JB.01726-08 (2009).

32 Peters, K. *et al.* The Redundancy of Peptidoglycan Carboxypeptidases Ensures Robust Cell Shape Maintenance in Escherichia coli. *MBio* **7**, doi:10.1128/mBio.00819-16 (2016).

33 Choi, J. & Groisman, E. A. Acidic pH sensing in the bacterial cytoplasm is required for Salmonella virulence. *Mol Microbiol* **101**, 1024-1038, doi:10.1111/mmi.13439 (2016).

34 Olsen, K. N. *et al.* Noninvasive measurement of bacterial intracellular pH on a single-cell level with green fluorescent protein and fluorescence ratio imaging microscopy. *Applied and environmental microbiology* **68**, 4145-4147 (2002).

35 Chakraborty, S., Mizusaki, H. & Kenney, L. J. A FRET-based DNA biosensor tracks OmpR-dependent acidification of Salmonella during macrophage infection. *PLoS Biol* **13**, e1002116, doi:10.1371/journal.pbio.1002116 (2015).

36 Ricke, S. C. Perspectives on the use of organic acids and short chain fatty acids as antimicrobials. *Poult Sci* **82**, 632-639, doi:10.1093/ps/82.4.632 (2003).

37 Krulwich, T. A., Sachs, G. & Padan, E. Molecular aspects of bacterial pH sensing and homeostasis. *Nat Rev Microbiol* **9**, 330-343, doi:10.1038/nrmicro2549 (2011).

38 Maggi, N., Pasqualucci, C. R., Ballotta, R. & Sensi, P. Rifampicin: a new orally active rifamycin. *Chemotherapy* **11**, 285-292, doi:10.1159/000220462 (1966).

39 McFarland, J. W. *et al.* Quantitative structure-activity relationships among macrolide antibacterial agents: in vitro and in vivo potency against Pasteurella multocida. *J Med Chem* **40**, 1340-1346, doi:10.1021/jm960436i (1997).

40 Jacobson, A. *et al.* A Gut Commensal-Produced Metabolite Mediates Colonization Resistance to Salmonella Infection. *Cell Host Microbe* **24**, 296-307 e297, doi:10.1016/j.chom.2018.07.002 (2018).

41 Komora, N., Bruschi, C., Magalhaes, R., Ferreira, V. & Teixeira, P. Survival of Listeria monocytogenes with different antibiotic resistance patterns to food-associated stresses. *Int J Food Microbiol* **245**, 79-87, doi:10.1016/j.ijfoodmicro.2017.01.013 (2017).

42 McMahon, M. A., Xu, J., Moore, J. E., Blair, I. S. & McDowell, D. A. Environmental stress and antibiotic resistance in food-related pathogens. *Applied and environmental microbiology* **73**, 211-217, doi:10.1128/AEM.00578-06 (2007).

43 O'Sullivan, E. & Condon, S. Intracellular pH is a major factor in the induction of tolerance to acid and other stresses in Lactococcus lactis. *Applied and environmental microbiology* **63**, 4210-4215 (1997).

44 Nicholson, J. K. *et al.* Host-gut microbiota metabolic interactions. *Science* **336**, 1262-1267, doi:10.1126/science.1223813 (2012).

45 Maier, L. *et al.* Extensive impact of non-antibiotic drugs on human gut bacteria. *Nature* **555**, 623-628, doi:10.1038/nature25979 (2018).

46 Beppler, C. *et al.* When more is less: Emergent suppressive interactions in three-drug combinations. *BMC Microbiol* **17**, 107, doi:10.1186/s12866-017-1017-3 (2017).

47 Fadrosh, D. W. *et al.* An improved dual-indexing approach for multiplexed 16S rRNA gene sequencing on the Illumina MiSeq platform. *Microbiome* **2**, 6, doi:10.1186/2049-2618-2-6 (2014).

48 Koch, M. A. *et al.* Maternal IgG and IgA Antibodies Dampen Mucosal T Helper Cell Responses in Early Life. *Cell* **165**, 827-841, doi:10.1016/j.cell.2016.04.055 (2016).

49 Hildebrand, F., Tadeo, R., Voigt, A. Y., Bork, P. & Raes, J. LotuS: an efficient and user-friendly OTU processing pipeline. *Microbiome* **2**, 30, doi:10.1186/2049-2618-2-30 (2014).

50 Salter, S. J. *et al.* Reagent and laboratory contamination can critically impact sequence-based microbiome analyses. *BMC Biol* **12**, 87, doi:10.1186/s12915-014-0087-z (2014).

51 Moens, F., Lefeber, T. & De Vuyst, L. Oxidation of metabolites highlights the microbial interactions and role of Acetobacter pasteurianus during cocoa bean fermentation. *Applied and environmental microbiology* **80**, 1848-1857, doi:10.1128/AEM.03344-13 (2014).

52 Zwietering, M. H., Jongenburger, I., Rombouts, F. M. & van 't Riet, K. Modeling of the bacterial growth curve. *Applied and environmental microbiology* **56**, 1875-1881 (1990).

53 Edelstein, A., Amodaj, N., Hoover, K., Vale, R. & Stuurman, N. *Computer Control of Microscopes Using μManager*. (John Wiley & Sons, Inc., 2010).

54 Ursell, T. *et al.* Rapid, precise quantification of bacterial cellular dimensions across a genomic-scale knockout library. *BMC biology* **15**, 17 (2017).

55 Stylianidou, S., Brennan, C., Nissen, S. B., Kuwada, N. J. & Wiggins, P. A. SuperSegger: robust image segmentation, analysis and lineage tracking of bacterial cells. *Mol Microbiol* **102**, 690-700, doi:10.1111/mmi.13486 (2016).

56 Marx, C. J. & Lidstrom, M. E. Development of improved versatile broad-host-range vectors for use in methylotrophs and other Gram-negative bacteria. *Microbiology* **147**, 2065-2075, doi:10.1099/00221287-147-8-2065 (2001).

57 Gibson, D. G. *et al.* Enzymatic assembly of DNA molecules up to several hundred kilobases. *Nature Methods* **6**, 343-345, doi:10.1038/nmeth.1318 (2009).

58 Deeraksa, A. *et al.* Characterization and spontaneous mutation of a novel gene, polE, involved in pellicle formation in Acetobacter tropicalis SKU1100. *Microbiology* **151**, 4111-4120, doi:10.1099/mic.0.28350-0 (2005).

59 Spath, K., Heinl, S., Egger, E. & Grabherr, R. *Lactobacillus plantarum* and *Lactobacillus buchneri* as expression systems: evaluation of different origins of replication for the design of suitable shuttle vectors. *Mol Biotechnol* **52**, 40-48 (2012).

60 Spath, K., Heinl, S. & Grabherr, R. "Direct cloning in Lactobacillus plantarum: electroporation with non-methylated plasmid DNA enhances transformation efficiency and makes shuttle vectors obsolete". *Microb Cell Fact* **11**, 141, doi:10.1186/1475-2859-11-141 (2012).